2018 Annual American Control Conference (ACC)
June 27–29, 2018. Wisconsin Center, Milwaukee, USA

An integral quadratic constraint framework for real-time steady-state optimization of linear time-invariant systems*

Zachary E. Nelson and Enrique Mallada

Abstract— **Achieving optimal steady-state performance in real-time is an increasingly necessary requirement of many critical infrastructure systems. In pursuit of this goal, this paper builds a systematic design framework of feedback controllers for Linear Time-Invariant (LTI) systems that continuously track the optimal solution of some predefined optimization problem. We logically divide the proposed solution into three components. The first component estimates the system state from the output measurements. The second component uses the estimated state and computes a drift direction based on an optimization algorithm. The third component calculates an input to the LTI system that aims to drive the system toward the optimal steady-state.**

We analyze the equilibrium characteristics of the closed-loop system and provide conditions for optimality and stability. Our analysis shows that the proposed solution guarantees optimal steady-state performance, even in the presence of constant disturbances. Furthermore, by leveraging recent results on the analysis of optimization algorithms using Integral Quadratic Constraints (IQCs), the proposed framework can translate input-output properties of our optimization component into sufficient conditions, based on linear matrix inequalities (LMIs), for global exponential asymptotic stability of the closed-loop system. We illustrate several resulting controller designs using a numerical example.

I. Introduction

Infrastructure systems are the foundation of our modern society. The Internet, power grids, and transportation networks are just some examples of the several critical systems that our current lifestyle relies on. Due to their large scale, the operational and fault-associated costs that these systems incur are both in the range of hundreds of millions of dollars to several billion dollars [1]. Therefore, operators continuously face the conflicting tasks of operating these systems as efficiently as possible and guaranteeing certain levels of security or robustness are maintained.

Traditionally, this balancing between efficiency and security is achieved by separating tasks across different time-scales. Efficiency goals are met using optimization algorithms running at a slow time-scale, and stability/robustness goals are attained using fast time-scale controllers. In power systems, for example, generators are optimally scheduled by solving an economic dispatch optimization problem at a slow time-scale (every 5/15 minutes, hour, or day) [2], whereas fast time-scale controllers based on frequency measurements [3] focus on preserving the system stability [4], not efficiency.

Unfortunately, the state of flux that these infrastructure systems currently experience due to the growing population, deployment of sensing and communication technologies, and sustainability trends, is pushing system operation towards its limits, and therefore rendering this traditional approach obsolete. Operating at maximum capacity does not leave room for the inefficiencies incurred by the timescale separation. Moreover, the limited coordination capabilities that today's controllers provide –when compared with optimization algorithms– does not allow the system to react to unprescribed events quickly. Motivated by this problem, this paper aims to remove the time-scale separation by building controllers that can simultaneously achieve steady-state optimality while preserving the system stability.

More precisely, this paper proposes a systematic design framework for feedback controllers that, given an LTI system and an unconstrained optimization problem, generates a family of nonlinear controllers that seek to drive the system towards the optimal solution of the optimization problem. Our equilibrium analysis gives a criterion for steady-state optimality of the closed-loop equilibrium. Furthermore, we leverage recent studies of optimization algorithms using Integral Quadratic Constraints (IQCs) [5], [6], [7] to provide sufficient conditions, based on Linear Matrix Inequalities [8], that guarantee global exponential asymptotic stability. The derived LMIs provide an explicit bound on the rate of convergence and allow us to design an algorithm that computes the maximum rate of convergence.

Our controllers have two main distinctive features. Firstly, they can be functionally separated into three components/modules: (i) an Estimator, that aims to estimate the system's state from the output; (ii) an Optimizer, that uses the estimated state to compute the drift direction necessary to achieve optimality or outputs zero when the estimated state is optimal; and (iii) a Driver (PI controller) that generates the necessary input to drive the system toward the optimal solution. Secondly, the Optimizer module can be implemented using one of many optimization algorithms, leading to a family of optimization-based nonlinear controllers. The only required conditions are that (i) in steady-state the output of the optimizer is zero if and only if its input (the estimated state) is the optimal solution of the optimization problem, and (ii) there exists an IQC that captures the input-output relationship of the optimizer.

Related Work: Optimization-based control design for achieving optimal steady-state performance has a been a popular subject of research for more than three decades. It has been

*This work was supported by the Army Research Office contract W911NF-17-1-0092, NSF grants (CNS 1544771, EPCN 1711188), and Johns Hopkins WSE startup funds.

Zachary E. Nelson and Enrique Mallada are with the Department of Electrical and Computer Engineering, The Johns Hopkins University, 3400 N. Charles Street, Baltimore, MD 21218, emails: {znelson2,mallada}@jhu.edu

used in communication networks to reverse engineer TCP/IP congestion control protocols [9], [10] and provide a design framework for novel congestion control algorithms [11], distributed multi-path routing [12], [13], and admission control [14], and access control in wireless networks [15]. In the context of power systems, optimization-based control design has been used for the design of distributed controllers that can achieve efficient supply-demand balance [16], frequency restoration [17], congestion management [18], and economic steady-state optimality [19], [20], [21]. Some of these approaches have been further extended to more general settings such as [22] and [23]. In general, these solutions either require that the dynamical system to be optimized has a specific structure, such as being passive [18], [19], having primal-dual dynamics [17], [21], [23], or having direct access to a subset of the system state [22].

More recently, real-time optimization algorithms have been proposed as a method to mitigate the substantial fluctuations that renewable energy introduces in power networks. The solutions fall within two categories depending on whether the system dynamics are considered as perturbations of the optimization algorithms [24], [25], or the system is modeled as a set of nonlinear algebraic constraints with slowly time-varying parameters [26], [27]. Our work distinguishes from these works by explicitly modeling the system dynamics and simultaneously guaranteeing the stability of the dynamical system and convergence to the optimal solution. Notably, while our framework today does not include optimization constraints or nonlinearities in the system dynamics, extending our framework to incorporate these features is the subject of our current research.

Paper Organization: The organization of the paper is as follows. Section II gives the reader preliminary tools that are necessary for the later analysis. Section III sets up the problem and discusses some of the challenges. Section IV proposes a design framework of controllers that address the challenges. Section V shows the systematic procedure for analyzing steady-state optimality and stability. Section VI considers a numerical example to illustrate the practicality of this approach. Lastly, Section VII summarizes the major points of the paper and suggests future work.

II. Preliminaries

A. Notation

The following notation will be used throughout the remainder of the paper. The $n \times n$ identity matrix is denoted as I_n. The $m \times n$ zero matrix is denoted as $\mathbb{0}_{m\times n}$. The zero vector with length n is denoted as $\mathbb{0}_n$. The subscripts are removed when the dimensions are implied by context. A positive (semi) definite matrix $P \in \mathbb{R}^{n\times n}$ is denoted as $P \succ 0$ ($\succeq 0$). All norms $||\cdot|| : \mathbb{R}^n \to \mathbb{R}$ are the standard ℓ_2-norm. The Kronecker product of two matrices is denoted by the symbol $\otimes$.

B. Integral Quadratic Constraints

Given a nonlinear mapping $\phi : p \mapsto q$, with $p, q \in \mathbb{R}^n$, and an input-output reference $(p_*, \phi(p_*)) \in \mathbb{R}^n \times \mathbb{R}^n$, we consider the class of pointwise IQCs.

Definition 1: The mapping ϕ is said to satisfy the *pointwise IQC* defined by $(Q_\phi, p_*, \phi(p_*))$ if

$$\begin{bmatrix} p - p_* \\ \phi(p) - \phi(p_*) \end{bmatrix}^T Q_\phi \begin{bmatrix} p - p_* \\ \phi(p) - \phi(p_*) \end{bmatrix} \geq 0$$

holds for all $(p, p_*) \in \mathbb{R}^n \times \mathbb{R}^n$, where $Q_\phi^T = Q_\phi \in \mathbb{R}^{2n\times 2n}$ is an indefinite matrix.

Next, we discuss two particular choices of the nonlinear map ϕ that are commonly used in optimization algorithms.

Gradient Mapping:
One source of nonlinearity that commonly arises in optimization algorithms is the gradient $\nabla f(p)$ of a function $f : \mathbb{R}^n \to \mathbb{R}$. In particular, characterizing the input-output properties of the gradient of a strongly convex function with a Lipschitz continuous gradient is of interest.

Definition 2: The gradient mapping $\nabla f : \mathbb{R}^n \to \mathbb{R}^n$ is *Lipschitz continuous* with parameter L if

$$||\nabla f(p) - \nabla f(p_*)|| \leq L||p - p_*||$$

holds for all $(p, p_*) \in \mathbb{R}^n \times \mathbb{R}^n$, where $L \geq 0$.

Definition 3: The function $f : \mathbb{R}^n \to \mathbb{R}^n$ is said to be *strongly convex* if

$$(\nabla f(p) - \nabla f(p_*))^T (p - p_*) \geq m||p - p_*||^2$$

holds for all $(p, p_*) \in \mathbb{R}^n \times \mathbb{R}^n$, where $m > 0$.

Using these two properties, it is possible to show that ∇f satisfies the pointwise IQC $(Q_f, p_*, \nabla f(p_*))$ defined by the matrix

$$Q_f := \begin{bmatrix} -2mL & L + m \\ L + m & -2 \end{bmatrix} \otimes I_n.$$

We refer the reader to [5] or [28] for a proof of this statement.

Proximal Mapping:
The second type of nonlinearity that will be used in this paper arises from the proximal mapping of a function.

Definition 4: The *proximal mapping* $\Pi_{\rho f} : \mathbb{R}^n \to \mathbb{R}^n$ of the function $f : \mathbb{R}^n \to \mathbb{R}$ with real parameter $\rho > 0$ is defined as

$$\Pi_{\rho f}(p) := \arg\min_{v\in\mathbb{R}^n} f(v) + \frac{1}{2\rho}||v - p||^2. \tag{1}$$

The optimality condition of (1) is:

$$\mathbb{0} = \nabla f(\Pi_{\rho f}(p)) + \frac{1}{\rho}(\Pi_{\rho f}(p) - p). \tag{2}$$

From (2), the proximal mapping can be viewed as the composition of the gradient mapping with an affine operator, followed by an inversion operation:

$$\Pi_{\rho f}(p) = (I + \rho\nabla f)^{-1}(p).$$

A known result is that $\Pi_{\rho f}$ satisfies the pointwise IQC $(Q_{\Pi_{\rho f}}, p_*, \Pi_{\rho f}(p_*))$ defined by the matrix

$$Q_{\Pi_{\rho f}} := \Big(\begin{bmatrix} 0 & \rho^{-1} \\ 1 & -\rho^{-1} \end{bmatrix} \otimes I_n \Big) Q_f \Big(\begin{bmatrix} 0 & 1 \\ \rho^{-1} & -\rho^{-1} \end{bmatrix} \otimes I_n \Big).$$

This result can be derived by using Lemma 1 followed by an IQC for inversion operations [6]. The proximal mapping is also know as the Moreau envelope. We refer the reader to [29] for additional background.

Affine Composition of IQCs:
The following lemma, whose proof can be found in [6], shows how to derive IQCs when a nonlinearity ϕ is composed with an affine map.

Lemma 1: (IQC for Affine Operations) Consider the nonlinear mapping ϕ that satisfies the pointwise IQC defined by $(Q_\phi, p_*, \phi(p_*))$. Define the affine mapping $\psi : \mathbb{R}^n \to \mathbb{R}^n$ to be $\psi(p) := S_2 p + S_1 \phi(S_0 p)$ where $S_0, S_1, S_2 \in \mathbb{R}^{n\times n}$ and S_1 is invertible. Then, ψ satisfies the pointwise IQC defined by $(Q_\psi, p_*, \psi(p_*))$, where

$$Q_\psi := \begin{bmatrix} S_0^T & -(S_1^{-1}S_2)^T \\ \mathbb{0}_{n\times n} & (S_1^{-1})^T \end{bmatrix} Q_\phi \begin{bmatrix} S_0 & \mathbb{0}_{n\times n} \\ -S_1^{-1}S_2 & S_1^{-1} \end{bmatrix}.$$

Stability Analysis Using IQCs:

The following lemma is useful when deriving stability conditions in terms of a LMI. See [8] and [30] for details.

Lemma 2: (Lossless S-Lemma) Let $A^T = A \in \mathbb{R}^{n\times n}$ and $B^T = B \in \mathbb{R}^{n\times n}$. Then, $A \succeq \sigma B$ holds for some $\sigma \geq 0$ if and only if $x^T B x \geq 0 \implies x^T A x \geq 0$ for all $x \in \mathbb{R}^n$.

We will now show how the input-output properties of an IQC can be used to generate a sufficient stability condition for the feedback interconnection of a LTI system and nonlinearity ϕ.

Proposition 1: Consider a LTI system defined by the matrices $\hat{A} \in \mathbb{R}^{n\times n}$, $\hat{B} \in \mathbb{R}^{n\times m}$, $\hat{C} \in \mathbb{R}^{m\times n}$, and $\hat{D} \in \mathbb{R}^{m\times m}$ with state $\xi \in \mathbb{R}^n$, input $q \in \mathbb{R}^m$, and output $p \in \mathbb{R}^m$:

$$\begin{aligned} \dot{\xi}(t) &= \hat{A}\xi(t) + \hat{B}q(t) \\ p(t) &= \hat{C}\xi(t) + \hat{D}q(t). \end{aligned}$$

Suppose the LTI system has the nonlinearity $\phi : \mathbb{R}^m \to \mathbb{R}^m$ as feedback so that $q = \phi(\hat{C}\xi + \hat{D}q)$. Assume ϕ satisfies the pointwise IQC $(Q_\phi, p_*, \phi(p_*))$ and the feedback interconnection is well-posed.[1] Then, the closed-loop equilibrium point $\xi_* \in \mathbb{R}^n$ has global exponential asymptotic stability of at least rate α if the LMI

$$\begin{bmatrix} \hat{A}^T P + P\hat{A} + \alpha P & P\hat{B} \\ \hat{B}^T P & \mathbb{0} \end{bmatrix} + \sigma \begin{bmatrix} \hat{C}^T & \mathbb{0} \\ \hat{D}^T & I_n \end{bmatrix} Q_\phi \begin{bmatrix} \hat{C} & \hat{D} \\ \mathbb{0} & I_n \end{bmatrix} \preceq 0 \tag{3}$$

is feasible for some $\sigma \geq 0$, $\alpha > 0$, and $P \succ 0$.

Proof: Assume that (3) is feasible. Let $\delta\xi := \xi - \xi_*$ and $\delta q := q - q_*$, where q_* is the input that achieves equilibrium. Consider the quadratic function $V(\delta\xi) = (\delta\xi)^T P \delta\xi$, where $P \in \mathbb{R}^{n\times n}$, $P \succ 0$. Lyapunov theory states that if V satisfies:

- $V(\mathbb{0}) = 0$ and $V(\delta\xi) > 0$ for all $\delta\xi \neq \mathbb{0}$,
- if $||\delta\xi|| \to \infty$, then $V(\delta\xi) \to \infty$ (radially unbounded),
- $\dot{V}(\delta\xi) \leq -\alpha V(\delta\xi)$ for all $\delta\xi \in \mathbb{R}^n$ and $\alpha > 0$,

then the equilibrium point has global exponential asymptotic stability of at least rate α [31].

Clearly, $V(\mathbb{0}) = 0$ and $V(\delta\xi) > 0, \forall \delta\xi \neq \mathbb{0}$ hold because $P \succ 0$. The radial unboundedness property similarly follows from $P \succ 0$. Using the fact that $\hat{A}\xi_* + \hat{B}q_* = \mathbb{0}$, the third property can be expressed as

$$\begin{aligned} &\dot{V}(\delta\xi) + \alpha V(\delta\xi) = 2(\delta\xi)^T P \dot{\delta\xi} + \alpha(\delta\xi)^T P \delta\xi \\ &= 2(\delta\xi)^T P((\hat{A}\xi + \hat{B}q) - (\hat{A}\xi_* + \hat{B}q_*)) + \alpha(\delta\xi)^T P\delta\xi \\ &= 2(\delta\xi)^T P(\hat{A}\delta\xi + \hat{B}\delta q) + \alpha(\delta\xi)^T P\delta\xi \\ &= (\delta\xi)^T P(\hat{A}\delta\xi + \hat{B}\delta q) + (\hat{A}\delta\xi + \hat{B}\delta q)^T P\delta\xi + \alpha(\delta\xi)^T P\delta\xi \\ &= \begin{bmatrix} \delta\xi \\ \delta q \end{bmatrix}^T \begin{bmatrix} \hat{A}^T P + P\hat{A} + \alpha P & P\hat{B} \\ \hat{B}^T P & \mathbb{0} \end{bmatrix} \begin{bmatrix} \delta\xi \\ \delta q \end{bmatrix} \leq 0. \end{aligned} \tag{4}$$

Finally, since the pointwise IQC $(Q_\phi, p_*, \phi(p_*)$ is satisfied,

$$\begin{bmatrix} \delta\xi \\ \delta q \end{bmatrix}^T \begin{bmatrix} \hat{C}^T & \mathbb{0} \\ \hat{D}^T & I_n \end{bmatrix} Q_\phi \begin{bmatrix} \hat{C} & \hat{D} \\ \mathbb{0} & I_n \end{bmatrix} \begin{bmatrix} \delta\xi \\ \delta q \end{bmatrix} \geq 0. \tag{5}$$

Since (3) is feasible and (5) holds, it directly follows from Lemma 2 that (4) holds. Hence, the equilibrium ξ_* has global exponential asymptotic stability of at least rate α. ■

III. Problem Setup

The problem setup is illustrated in Fig. 1, where we consider a LTI system represented by a state-space model where $x \in \mathbb{R}^n$ is the state, $u \in \mathbb{R}^m$ is the input, and $y \in \mathbb{R}^p$ is the output:

$$\begin{aligned} \dot{x}(t) &= Ax(t) + Bu(t) \\ y(t) &= Cx(t) + Du(t). \end{aligned} \tag{6}$$

The input $u(t)$ is the sum of a control signal $r(t) \in \mathbb{R}^m$ and an unknown constant disturbance $w(t) = w \in \mathbb{R}^m$, i.e. $u(t) = w(t) + r(t) = w + r(t)$. Ideally, a disturbance on the measurement $y(t)$ should also be considered and is a current topic of our research. Finally, the feedback operator $\Psi(\cdot)$ denotes the (possibly nonlinear) feedback control to be designed.

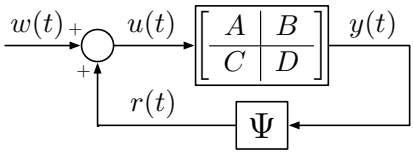

Fig. 1. LTI system interconnected with a nonlinear mapping and constant disturbance signal.

Our goal is to, given the measurement y, design a control input $r = \Psi(y)$ that drives the system (6) to a steady-state x_* that is an optimal solution of a predefined optimization problem

$$\min_{x\in\mathbb{R}^n} f(x), \tag{7}$$

where $f : \mathbb{R}^n \to \mathbb{R}$ is a given cost function.

Therefore, given the measurement $y(t)$, the feedback $\Psi(\cdot)$ must produce a control $r = \Psi(y)$ such that $x(t) \to \mathcal{X}^*$, where $\mathcal{X}^*$ is the set of optimal solutions to (7), i.e.,

$$\mathcal{X}^* = \{x \in \mathbb{R}^n : \nabla f(x) = \mathbb{0}\}.$$

Throughout this paper we make the following assumption.

Assumption 1: The cost function $f(x)$ of the optimization problem (7) is continuously differentiable, strongly convex,

[1]The definition of well-posedness is given in Section III.

and has a Lipschitz continuous gradient. This implies that the set $\mathcal{X}^*$ is a singleton.[2]

Finally, we provide a concrete model for $\Psi(\cdot)$. As the optimality conditions for optimization problem (7) are in general nonlinear, the feedback controllers to be designed will be necessarily of the same type. Thus, we consider the nonlinear feedback Ψ using the nonlinear dynamics

$$\Psi: \quad \begin{aligned} \dot{\eta}(t) &= F(\eta(t), y(t)) \\ r(t) &= H(\eta(t), y(t)), \end{aligned} \tag{8}$$

where $\eta \in \mathbb{R}^d$ is the state of the feedback dynamics, $r \in \mathbb{R}^m$ is the output of the feedback dynamics, and the mappings $F : \mathbb{R}^d \times \mathbb{R}^p \to \mathbb{R}^d$ and $H : \mathbb{R}^d \times \mathbb{R}^p \to \mathbb{R}^m$ are possibly nonlinear.

Remark 1 (Well-Posedness): From the feedthrough terms present in (6) and (8), it is possible a priori that the feedback interconnection is not well-posed.[3] A sufficient condition that prevents this problem is by enforcing that whenever $D \neq \mathbb{0}$, the map H depends only on η, i.e., $r(t) = H(\eta(t))$. We will further discuss this condition in Section IV.

A. Design Challenges

There are several challenges associated to designing (8) such that in steady-state, $x_* \in \mathcal{X}^*$.

- *Lack of direct access to $x(t)$:* The system output matrix C is not necessarily invertible. Thus, recovering $x(t)$ from $y(t)$ is not straightforward.
- *Finding the solution $x_* \in \mathcal{X}^*$:* Finding the optimal solution to (7) is usually challenging or the cost function may change, giving not enough time to recompute x_*.
- *Driving $x(t)$ to $x_* \in \mathcal{X}^*$:* Even if one has access to the optimal solution x_*, one then needs to design the correct $r(t)$ that ensures that $x(t)$ converges to it.

Interestingly, some of these challenges can be easily handled using tools from control theory, such as recovering $x(t)$ from $y(t)$ or driving $x(t)$ to x_*. On the other hand, finding an optimal solution x_* is the major goal within optimization theory. Therefore, when the timescale of the control and optimization tasks do not intersect, our problem can be easily solved using standard tools from control and optimization. However, when the timescale separation is no longer present, the problem becomes more challenging as there are no standard tools to address it. This problem is systematically addressed in the next section.

IV. Optimization-Based Control Design

In this section we describe the proposed optimization-based controllers, that combine tools from control and optimization, and leverage the IQC framework described in the preliminaries. The crux of our solution is a modularized architecture that breaks down the feedback dynamics (8) into three serial components that systematically addresses the challenges described in the previous section and allow a straightforward application of Proposition 1 to certify global exponential asymptotic stability.

[2]Relaxing this assumption is desired and is a subject of future work.

[3]The feedback interconnection of (6) and (8) is well-posed if $u(t)$ and $y(t)$ are uniquely defined for every choice of states $x(t)$ and $\eta(t)$.

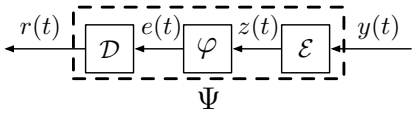

Fig. 2. Optimization-based control feedback breakdown.

The proposed architecture is described in Fig. 2. The first component $\mathcal{E} : y(t) \mapsto z(t)$ is a state *estimator* that takes the output of the LTI system and produces a state estimate $z(t)$. The second component $\varphi : z(t) \mapsto e(t)$, referred to as the *optimizer*, takes the state estimate and produces a measurement of the optimality error or direction of desired drift $e(t)$, which is required to be zero if and only if the input is in the set $\mathcal{X}^*$. The optimizer can be thought of as the part of optimization algorithm that dictates the direction of the next step. The third component $\mathcal{D} : e(t) \mapsto r(t)$, the *driver*, takes the optimality error and produces the input to the LTI system that ensures that the equilibrium satisfies $e_* = \mathbb{0}$.

Remark 2: One of the advantages of the proposed architecture is the role independence of each component. This allows for a subsystem to be skipped if the functionality is not required. For example, in cases where $y(t) = x(t)$ or the optimization problem uniquely depends on $y(t)$, then the estimator block can be avoided.

In the remainder of this section, we describe the design requirements of each proposed component/subsystem and give examples on how to implement them.

A. Design of the Estimator $\mathcal{E}$

The estimator component $\mathcal{E} : y(t) \mapsto z(t)$ is perhaps the simplest to design. Its goal to build an estimate of the state, $z(t)$, from $y(t)$. The design requirement of $\mathcal{E}$ is:

- **A.1:** If the dynamics of (6) are in equilibrium, then the dynamics of $\mathcal{E}$ are in equilibrium if and only if $z_* = x_*$.

Therefore, an obvious choice for $\mathcal{E}$ is an observer/state estimator. The dynamics of $\mathcal{E}$ are given by

$$\mathcal{E}: \quad \begin{aligned} \dot{\hat{x}} &= (A - LC)\hat{x} + (B - LD)u + Ly \\ z &= \hat{x}, \end{aligned}$$

where $L \in \mathbb{R}^{n \times p}$ is a matrix to be designed.

A standard argument for observers shows that the evolution of the error $\delta x(t) := x(t) - z(t)$ is given by

$$\dot{\delta x}(t) = (A - LC)\delta x(t).$$

Moreover, if (6) is observable, L can be chosen to satisfy

$$\text{rank}(A - LC) = n. \tag{9}$$

B. Design of the Optimizer φ

The optimizer φ has two design requirements:

- **B.1:** The optimizer must take the estimated state $z(t)$ to produce a measure of optimality error or direction of drift $e(t)$ such that $e_* = \mathbb{0}$ if and only if $z_* \in \mathcal{X}^*$.
- **B.2:** The input-output characteristics of φ must be captured by an IQC $(Q_\varphi, z_*, \varphi(z_*))$.

For the purpose of this paper, we consider two possible solutions.

φ_1: Gradient Descent. The first solution considered is the standard gradient descent mapping, i.e.,

$$\varphi_1 := -\nabla f. \tag{10}$$

It is straightforward to verify that requirement B.1 holds. The following lemma explicitly computes the IQC for φ_1.

Lemma 3: Assume the pointwise IQC $(Q_f, z_*, \nabla f(z_*))$ is satisfied. Then, the pointwise IQC $(Q_{\varphi_1}, z_*, \varphi_1(z_*))$ defined by the matrix

$$Q_{\varphi_1} := \Big(\begin{bmatrix} 1 & 0 \\ 0 & -1 \end{bmatrix} \otimes I_n \Big) Q_f \Big(\begin{bmatrix} 1 & 0 \\ 0 & -1 \end{bmatrix} \otimes I_n \Big)$$

is satisfied.

Proof: The IQC immediately follows from Lemma 1 with $\phi = \nabla f$, $S_0 = I_n$, $S_1 = -I_n$, and $S_2 = \mathbb{0}_{n\times n}$. ∎

φ_2: Proximal Tracking. Our second option for the optimizer block is inspired by the proximal mapping (1). It essentially computes the error between the input $z(t)$ and the solution given by the proximal operator $\Pi_{\rho f}(z(t))$, that is,

$$\varphi_2 := \Pi_{\rho f} - I_n. \tag{11}$$

The following proposition shows that (11) satisfies the first design requirement.

Proposition 2: The mapping φ_2 satisfies B.1.

Proof: Assume that $e_* = \mathbb{0}$. Then from (11), we have that $\Pi_{\rho f}(z_*) = z_*$. It follows from (2) that

$$\mathbb{0} = \nabla f(\Pi_{\rho f}(z_*)) + \frac{1}{\rho}(\Pi_{\rho f}(z_*) - z_*) \iff \mathbb{0} = \nabla f(z_*).$$

By the definition of $\mathcal{X}^*$, $z_* \in \mathcal{X}^*$.

Conversely, assume that $z_* \in \mathcal{X}^*$. Since

$$\arg\min_{v\in\mathbb{R}^n} f(v) = z_* \text{ and } \arg\min_{v\in\mathbb{R}^n} \frac{1}{2\rho}||v - z_*||^2 = z_*,$$

it follows that $\Pi_{\rho f}(z_*) = z_*$. Thus, $e_* = \mathbb{0}$. ∎

The next lemma computes the IQC that characterizes φ_2.

Lemma 4: Assume the pointwise IQC $(Q_f, z_*, \nabla f(z_*))$ is satisfied. Then, the pointwise IQC $(Q_{\varphi_2}, z_*, \varphi_2(z_*))$ defined by the matrix

$$Q_{\varphi_2} := \Big(\begin{bmatrix} 1 & 1 \\ 0 & 1 \end{bmatrix} \otimes I_n \Big) Q_{\Pi_{\rho f}} \Big(\begin{bmatrix} 1 & 0 \\ 1 & 1 \end{bmatrix} \otimes I_n \Big).$$

is satisfied.

Proof: The IQC immediately follows from Lemma 1 with $\phi = \Pi_{\rho f}$, $S_0 = I_n$, $S_1 = I_n$, and $S_2 = -I_n$. ∎

C. Design of the Driver $\mathcal{D}$

The last component of the proposed solution is in charge of generating the control signal $r(t)$ that drives the system towards the optimal solution of (7). The design requirement for $\mathcal{D}$ is:

- **C.1:** The dynamics of $\mathcal{D}$ are in equilibrium if and only if $e_* = \mathbb{0}$.

Thus, one possible choice would be to use a Proportional-Integral (PI) controller defined by the dynamics

$$\mathcal{D}: \quad \dot{e}_I = e,\ r = K_I e_I + K_P e$$

where $K_I, K_P \in \mathbb{R}^{m\times n}$ are matrices to be designed.

It is simple to show that $\dot{e}_I = \mathbb{0}$ if and only if $e_* = \mathbb{0}$. In fact, this also shows that we only need an integrator to satisfy the design requirement. However, a PI controller provides better dynamic properties than a pure integrator and therefore we choose to add the proportional term.

D. Integrated System

This resulting interconnected system using the example design choices is shown in Fig. 3.

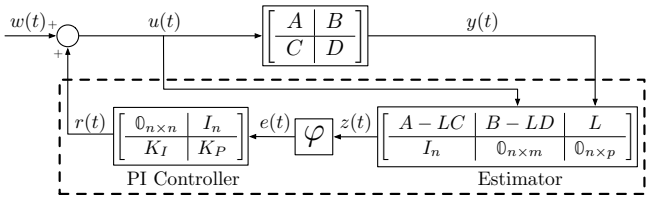

Fig. 3. LTI system in feedback with a state estimator $\mathcal{E}$, optimizer φ, and PI controller as the driver $\mathcal{D}$.

Remark 3: Whenever the estimator subsystem $\mathcal{E}$ is included in the interconnection, the feedback interconnection will be well-posed because $r(t)$ only depends on $\eta(t)$. However, well-posedness is not guaranteed when $D \neq \mathbb{0}$, $K_P \neq \mathbb{0}$, and there is no estimator subsystem because

$$r(t) = K_P\varphi(Cx(t) + D(w + r(t))) + K_I e_I(t)$$

depends on itself. One simple solution to overcome this issue is add a module $\mathcal{E}$ such that $z(t) = y(t) - Du(t)$.

The next section shows that indeed the integrated system is able to guarantee steady-state optimality under mild conditions and illustrates how the IQC framework can be leveraged to guarantee global exponential asymptotic stability.

V. Optimality and Convergence

A. Optimality Analysis

The optimality analysis requires the following assumption.

Assumption 2: The system is steady-state controllable. That is, given any steady-state x_*, there exists an input u_* such that $Ax_* + Bu_* = \mathbb{0}$.

Assumption 2 is in some sense *necessary* to ensure that the system can achieve an arbitrary steady-state. Although this assumption is stronger than the standard controllability assumption, we point out that while controllability is sufficient to drive $x(t)$ towards any state x_* in finite time, it does not requires that $x(t)$ remains equal to x_*.

Theorem 1: Suppose design requirements A.1, B.1, and C.1 are satisfied and Assumption 2 holds. Then, the point (x_*, z_*, e_{I*}) is an equilibrium point of the interconnected system if and only if $x_* \in \mathcal{X}^*$, $z_* = x_*$, $e_* = \mathbb{0}$, and $r_* = u_* - w$, where u_* satisfies $Ax_* + Bu_* = \mathbb{0}$.

Proof: Assume (x_*, z_*, e_{I*}) is an equilibrium point of the interconnected system. Since $\dot{e}_I = \mathbb{0}$, it follows from C.1 that $e_* = \mathbb{0}$. Furthermore, $\dot{e}_I = \mathbb{0}$ and $\dot{x} = \mathbb{0}$ together imply that $r_* = u_* - w$, where u_* satisfies $Ax_* + Bu_* = \mathbb{0}$. Since $e_* = \mathbb{0}$, it follows from B.1 that $z_* \in \mathcal{X}^*$. Lastly, since $\dot{x} = \mathbb{0}$ and $\hat{\dot{x}} = \mathbb{0}$, it follows from A.1 that $z_* = x_*$.

Conversely, assume that $x_* \in \mathcal{X}^*, z_* = x_*, e_* = \mathbb{0}$, and $r_* = u_* - w$, where u_* satisfies $Ax_* + Bu_* = \mathbb{0}$ (such a

u_* exists because of Assumption 2). It directly follows from $r_* = u^* - w$ that $\dot{x} = \mathbb{0}$. Since $e_* = \mathbb{0}$, it follows from C.1 that $\dot{e}_I = \mathbb{0}$. Since $\dot{x} = \mathbb{0}$ and $z_* = x_*$, it follows from A.1 that $\dot{\hat{x}} = \mathbb{0}$. Hence, (x_*, z_*, e_{I*}) is an equilibrium point of the interconnected system. ■

B. Stability Analysis

This section will derive a sufficient condition for the global exponential asymptotic stability of the equilibrium point considered in the optimality analysis. For this analysis, it is useful to group the linear dynamics of $\mathcal{E}$ and $\mathcal{D}$ into the LTI system to essentially create a larger dimension LTI system. The resulting system is

$$\dot{\xi} = \underbrace{\begin{bmatrix} A & \mathbb{0} & BK_I \\ LC & A - LC & BK_I \\ \mathbb{0} & \mathbb{0} & \mathbb{0} \end{bmatrix}}_{\hat{A}} \xi + \underbrace{\begin{bmatrix} BK_P \\ BK_P \\ I_n \end{bmatrix}}_{\hat{B}_e} e + \underbrace{\begin{bmatrix} B \\ B \\ \mathbb{0} \end{bmatrix}}_{\hat{B}_w} w$$

$$z = \underbrace{\begin{bmatrix} \mathbb{0} & I_n & \mathbb{0} \end{bmatrix}}_{\hat{C}} \xi, \text{where } \xi := \begin{bmatrix} x^T & \hat{x}^T & e_I^T \end{bmatrix}^T.$$

Theorem 2: Consider the interconnection of the LTI system (6) with the feedback controller specified in Fig. 3. Consider the equilibrium point (x_*, z_*, e_{I*}) characterized by Theorem 1. Assume B.2 holds so the pointwise IQC $(Q, z_*, \varphi(z_*))$ is satisfied. Then, the equilibrium point (x_*, z_*, e_{I*}) has global exponential stability of at least rate α if the LMI

$$\begin{bmatrix} \hat{A}^T P + P\hat{A} + \alpha P & P\hat{B}_e \\ \hat{B}_e^T P & \mathbb{0} \end{bmatrix} + \sigma \begin{bmatrix} \hat{C}^T & \mathbb{0} \\ \mathbb{0} & I_n \end{bmatrix} Q \begin{bmatrix} \hat{C} & \mathbb{0} \\ \mathbb{0} & I_n \end{bmatrix} \preceq 0 \tag{12}$$

is feasible for some $\sigma \geq 0, \alpha > 0$, and $P \succ 0$.

Proof: The proof is a direct application of Proposition 1 to the larger dimension LTI system. ■

C. Convergence Rate

Finally, we show how the LMI condition derived in Theorem 2 can be leveraged to compute the maximum convergence rate that the system can achieve. Our goal here is to solve the optimization problem:

$$\underset{\sigma \geq 0, \alpha > 0, P \succ 0}{\text{maximize}} \ \alpha \text{ subject to } (12). \tag{13}$$

The main challenge is that because α multiplies P in (12), the optimization problem is non-convex. However, for a fixed α, finding whether (12) is feasible can be done efficiently. Therefore, it is possible to implement a line search in α that finds the maximum value $\alpha_{\max}$ that satisfies (12).

VI. Numerical Example

The purpose of this section is to jointly compare the performance of the gradient and proximal optimizers on a simple MIMO system. We leave the more extensive numerical study for the journal version of this paper. The example we are interested in is a second order LTI system defined by

$$A = \begin{bmatrix} 0 & 1 \\ -10 & -5 \end{bmatrix}, \ B = \begin{bmatrix} 1 & 4 \\ 1 & 0 \end{bmatrix}, \ C = \begin{bmatrix} 1 & 0 \end{bmatrix}, \ D = \mathbb{0}_{1\times 2},$$

with $x, u \in \mathbb{R}^2$ and $y \in \mathbb{R}$. Since the output of the LTI system only has information about the first state, an estimator module is obviously needed. We choose the controller parameters as

$$K_I = K_P = \begin{bmatrix} 0 & 1 \\ 1/4 & -1/4 \end{bmatrix} \text{ and } L = \begin{bmatrix} 1 \\ 1 \end{bmatrix}.$$

A. Convergence Rate Optimization

We first find the solution of (13) as a function of ρ for the specified LTI system and controller. Several curves corresponding to different convexity and Lipschitz parameters are plotted in Fig. 4. With a sufficiently large ρ, φ_2 was able to achieve a larger $\alpha_{\max}$ than φ_1 when $m = 0.75$, but was not able to when $m = 1.25$. For both optimizer types, $L = 1.25$ resulted in a larger $\alpha_{\max}$ than $L = 1.5$.

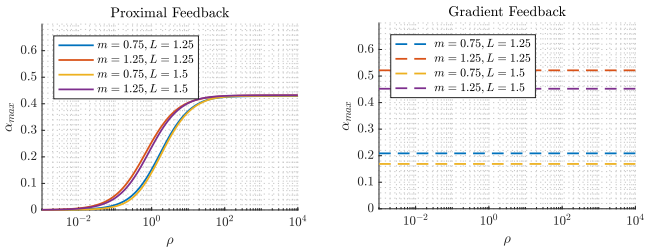

Fig. 4. Maximum feasible α versus ρ for several cost functions when using (a): φ_2 (proximal optimizer) and (b): φ_1 (gradient optimizer).

After choosing a sufficiently large ρ, the solution of (13) was plotted as a function of m and is shown in Fig. 5. The Lipschitz constant was chosen as multiples of m. The φ_1 optimizer resulted in a larger $\alpha_{\max}$ when L was chosen closer to m. Conversely, the φ_2 optimizer resulted in a larger $\alpha_{\max}$ when the multiple was chosen farther from m.

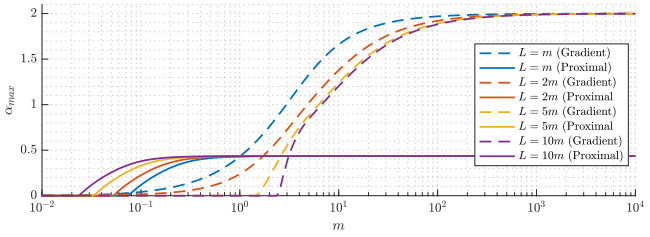

Fig. 5. Maximum feasible α versus m for several different choices of L when using φ_1 and φ_2 optimizers.

B. Closed-Loop System Simulation

Let the cost function of the optimization problem be

$$f(x) = \frac{1}{2} x^T \begin{bmatrix} 1 & 1/6 \\ 1/6 & 2/3 \end{bmatrix} x - \begin{bmatrix} 17/3 & 4/3 \end{bmatrix} x.$$

The Lipschitz constant is the larger eigenvalue of the quadratic matrix $L \approx 1.0690$ and the strong convexity constant is the smaller eigenvalue $m \approx 0.5976$. The optimal solution of the problem is $x_* \approx \begin{bmatrix} 5.5652 & 0.6087 \end{bmatrix}^T$.

The system's state trajectory for various optimizer choices is given in Fig. 6. The constant disturbance signal was

initially set to zero, but at $t = 75$s was changed to $w = \begin{bmatrix} 1 & 1 \end{bmatrix}^T$. All trajectories were able to recover from the change in disturbance and there were cases when φ_2 outperformed φ_1. It is particularly interesting that x_2 has the ability to reach the optimal solution despite the fact that it is not being measured.

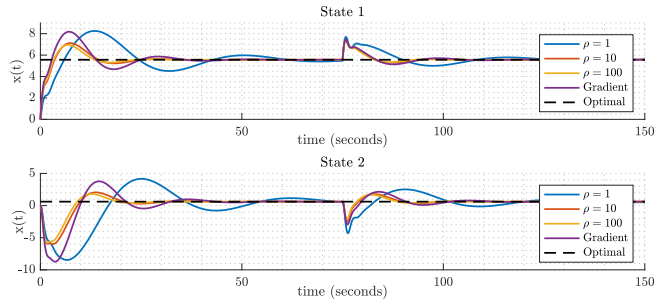

Fig. 6. System (a) state 1 and (b) state 2 versus time when using φ_1 and φ_2 optimizers. Several choices of ρ are shown for the φ_2 optimizer.

VII. Conclusions

This paper introduces a framework of nonlinear controllers whose purpose is to drive a given LTI system to the optimal solution of some predefined optimization problem. The controllers are composed of an *estimator*, *optimizer*, and *driver*. We give specific design requirements and possible design choices for each of these modules. Our analysis shows that under mild assumptions, we can guarantee optimal steady-state performance. Moreover, we give a sufficient LMI condition so that global exponential asymptotic stability of the optimal steady-state is guaranteed. Lastly, we present numerical illustrations that demonstrate how the design choices relate to the rate of exponential convergence. The main focus of future work includes further generalizing the proposed framework. In particular, we will consider constrained optimization problems, multiple distributed LTI systems, and performance tuning (i.e., how to choose controller parameters).

References

[1] R. J. Campbell, "Weather-related power outages and electric system resiliency." Congressional Research Service, Library of Congress Washington, DC, 2012.

[2] A. K. Bejestani, A. Annaswamy, and T. Samad, "A hierarchical transactive control architecture for renewables integration in smart grids: Analytical modeling and stability," *IEEE Transactions on Smart Grid*, vol. 5, no. 4, pp. 2054–2065, July 2014.

[3] A. J. Wood and B. F. Wollenberg, *Power generation, operation, and control*, 3rd ed. John Wiley & Sons, 2013.

[4] Ibraheem, P. Kumar, and D. P. Kothari, "Recent philosophies of automatic generation control strategies in power systems," *IEEE Transactions on Power Systems*, vol. 20, no. 1, pp. 346–357, Feb 2005.

[5] L. Lessard, B. Recht, and A. Packard, "Analysis and design of optimization algorithms via integral quadratic constraints," *SIAM Journal on Optimization*, vol. 26, no. 1, pp. 57–95, 2016.

[6] M. Fazlyab, A. Ribeiro, M. Morari, and V. M. Preciado, "Analysis of optimization algorithms via integral quadratic constraints: Nonstrongly convex problems," *arXiv preprint arXiv:1705.03615*, 2017.

[7] B. Hu and L. Lessard, "Control interpretations for first-order optimization methods," in *2017 American Control Conference (ACC)*, May 2017, pp. 3114–3119.

[8] S. Boyd, L. El Ghaoui, E. Feron, and V. Balakrishnan, *Linear Matrix Inequalities in System and Control Theory*, ser. Studies in Applied Mathematics. Philadelphia, PA: SIAM, Jun. 1994, vol. 15.

[9] F. P. Kelly, A. K. Maulloo, and D. K. H. Tan, "Rate control for communication networks: Shadow prices, proportional fairness and stability," *The Journal of the Operational Research Society*, vol. 49, no. 3, pp. 237–252, 1998.

[10] S. H. Low and D. E. Lapsley, "Optimization flow control. I. Basic algorithm and convergence," *IEEE/ACM Transactions on Networking*, vol. 7, no. 6, pp. 861–874, Dec 1999.

[11] D. X. Wei, C. Jin, S. H. Low, and S. Hegde, "FAST TCP: Motivation, Architecture, Algorithms, Performance," *IEEE/ACM Transactions on Networking*, vol. 14, no. 6, pp. 1246–1259, 2006.

[12] M. Q. Rieck, S. Pai, and S. Dhar, "Distributed routing algorithms for multi-hop ad hoc networks using d-hop connected d-dominating sets," *Computer Networks*, vol. 47, no. 6, pp. 785–799, 2005.

[13] E. Mallada and F. Paganini, "Stability of node-based multipath routing and dual congestion control," in *2008 47th IEEE Conference on Decision and Control*, Dec 2008, pp. 1398–1403.

[14] A. Ferragut and F. Paganini, "Achieving network stability and user fairness through admission control of TCP connections," in *2008 42nd Annual Conference on Information Sciences and Systems*, March 2008, pp. 1195–1200.

[15] L. Chen, S. H. Low, M. Chiang, and J. C. Doyle, "Cross-layer congestion control, routing and scheduling design in ad hoc wireless networks," in *25th IEEE International Conference on Computer Comunications*, 2006, pp. 1–13.

[16] C. Zhao, U. Topcu, N. Li, and S. Low, "Design and stability of load-side primary frequency control in power systems," *IEEE Transactions on Automatic Control*, vol. 59, no. 5, pp. 1177–1189, 2014.

[17] E. Mallada, C. Zhao, and S. H. Low, "Optimal load-side control for frequency regulation in smart grids," *IEEE Transactions on Automatic Control*, 6 2017.

[18] C. Zhao, E. Mallada, S. H. Low, and J. W. Bialek, "A unified framework for frequency control and congestion management," in *Power Systems Computation Conference*, 06 2016, pp. 1–7.

[19] F. Dörfler, J. Simpson-Porco, and F. Bullo, "Breaking the Hierarchy: Distributed Control & Economic Optimality in Microgrids," *IEEE Transactions on Control of Network Systems*, vol. 3, no. 3, pp. 241–253, 2016.

[20] A. Cherukuri and J. Cortés, "Distributed generator coordination for initialization and anytime optimization in economic dispatch," *IEEE Transactions on Control of Network Systems*, vol. 2, no. 3, pp. 226–237, Sept 2015.

[21] N. Li, C. Zhao, and L. Chen, "Connecting automatic generation control and economic dispatch from an optimization view," *IEEE Transactions on Control of Network Systems*, vol. 3, no. 3, pp. 254–264, Sept 2016.

[22] A. Jokic, M. Lazar, and P. P. J. van den Bosch, "On constrained steady-state regulation: Dynamic KKT controllers," *IEEE Transactions on Automatic Control*, vol. 54, no. 9, pp. 2250–2254, Sept 2009.

[23] X. Zhang, A. Papachristodoulou, and N. Li, "Distributed optimal steady-state control using reverse- and forward-engineering," in *2015 54th IEEE Conference on Decision and Control (CDC)*, Dec 2015, pp. 5257–5264.

[24] E. Dall'Anese and A. Simonetto, "Optimal power flow pursuit," *IEEE Transactions on Smart Grid*, 2016.

[25] E. Dall'Anese, S. V. Dhople, and G. B. Giannakis, "Photovoltaic inverter controllers seeking ac optimal power flow solutions," *IEEE Transactions on Power Systems*, vol. 31, no. 4, pp. 2809–2823, July 2016.

[26] F. Dörfler and S. Grammatico, "Amidst centralized and distributed frequency control in power systems," in *2016 American Control Conference (ACC)*, July 2016, pp. 5909–5914.

[27] Y. Tang, K. Dvijotham, and S. Low, "Real-time optimal power flow," *IEEE Transactions on Smart Grid*, 2017.

[28] Y. Nesterov, *Introductory Lectures on Convex Optimization: A Basic Course*, 1st ed. Springer Publishing Company, Incorporated, 2014.

[29] N. H. Dhingra, S. Z. Khong, and M. R. Jovanović, "The proximal augmented lagrangian method for nonsmooth composite optimization," *arXiv preprint arXiv:1610.04514*, 2016.

[30] K. Derinkuyu and M. Ç. Pınar, "On the s-procedure and some variants," *Mathematical Methods of Operations Research*, vol. 64, no. 1, pp. 55–77, 2006.

[31] H. K. Khalil, *Nonlinear systems; 3rd ed.* Upper Saddle River, NJ: Prentice-Hall, 2002.